JVSTB Journal of Vacuum Science & Technology B

Molecular beam epitaxial growth of high-reflectivity and broad-bandwidth ZnTe/GaSb distributed Bragg reflectors

Jin Fan, Xinyu Liu, Lu Ouyang, Richard E. Pimpinella, Margaret Dobrowolska, Jacek K. Furdyna, David J. Smith, and Yong-Hang Zhang

Citation: Journal of Vacuum Science & Technology B **31**, 03C109 (2013); doi: 10.1116/1.4793475
View online: http://dx.doi.org/10.1116/1.4793475
View Table of Contents: http://scitation.aip.org/content/avs/journal/jvstb/31/3?ver=pdfcov
Published by the AVS: Science & Technology of Materials, Interfaces, and Processing

Molecular beam epitaxial growth of high-reflectivity and broad-bandwidth ZnTe/GaSb distributed Bragg reflectors

Jin Fan
Center for Photonics Innovation, Arizona State University,Tempe, Arizona 85287 and School of Electrical, Computer, and Energy Engineering, Arizona State University, Tempe, Arizona 85287

Xinyu Liu
Department of Physics, University of Notre Dame, Notre Dame, Indiana 46556

Lu Ouyang
Center for Photonics Innovation, Arizona State University, Tempe, Arizona 85287 and Department of Physics, Arizona State University, Tempe, Arizona 85287

Richard E. Pimpinella, Margaret Dobrowolska, and Jacek K. Furdyna
Department of Physics, University of Notre Dame, Notre Dame, Indiana 46556

David J. Smith
Center for Photonics Innovation, Arizona State University, Tempe, Arizona 85287 and Department of Physics, Arizona State University, Tempe, Arizona 85287

Yong-Hang Zhang[a)]
Center for Photonics Innovation, Arizona State University, Tempe, Arizona 85287 and School of Electrical, Computer, and Energy Engineering, Arizona State University, Tempe, Arizona 85287

(Received 15 December 2012; accepted 12 February 2013; published 25 February 2013)

This paper reports the molecular beam epitaxial growth and characterization of high-reflectivity and broad-bandwidth distributed Bragg reflectors (DBRs) made of ZnTe/GaSb quarter-wavelength ($\lambda/4$) layers for optoelectronic applications in the midwave infrared spectral range (2–5 μm). A series of ZnTe/GaSb DBRs has been successfully grown on GaSb (001) substrates using molecular beam epitaxy (MBE). During the MBE growth, a temperature ramp was applied to the initial growth of GaSb layers on ZnTe to protect the ZnTe underneath from damage due to thermal evaporation. Post-growth characterization using high-resolution x-ray diffraction, atomic force microscopy, and transmission electron microscopy reveals smooth surface morphology, low defect density, and coherent interfaces. Reflectance spectroscopy results show that a DBR sample of seven $\lambda/4$ pairs has a peak reflectance as high as 99.0% centered at 2.56 μm with a bandwidth of 517 nm. © *2013 American Vacuum Society*. [http://dx.doi.org/10.1116/1.4793475]

I. INTRODUCTION

Midwave infrared (MWIR) laser diodes are of much interest for gas sensing and spectroscopic applications due to the strong absorption lines of various gases in the MWIR spectral range from 2 to 5 μm. It has been found that vertical-cavity surface-emitting lasers (VCSELs) are desirable laser sources offering many advantages, such as small beam divergence, single-mode operation, low threshold, and ease of monolithic integration with microelectromechanical system structure for wide wavelength tunability.[1–4] Much research has been done on InP- and GaSb-based VCSELs emitting in the near-infrared (NIR) and MWIR range.[5–8] While InP-based heterostructures have shown an emission wavelength limit up to 2.3 μm,[9] GaSb-based heterostructures allow coverage of a major part of the 2–4 μm range. Typical VCSELs use high-reflectivity mirrors, usually in the form of distributed Bragg reflectors (DBRs). However, it has been found that almost all III-V semiconductors lattice-matched to InP or GaSb have very small refractive index contrast, which makes it challenging to achieve high reflectivity using thin DBRs to reduce the VCSEL threshold current density. It is, therefore, highly desirable to develop a DBR structure lattice-matched to GaSb, which has high material quality, large refractive index contrast, and broad wavelength tunability, for monolithically integrated tunable VCSELs.

A DBR structure consisting of ZnTe and GaSb $\lambda/4$ layers has recently been proposed for the use in MWIR VCSELs (Ref. 10) and other optoelectronic applications. The ZnTe and GaSb semiconductors have lattice constants very close to 6.1 Å and a lattice mismatch of only 0.13%, which potentially offers unlimited degrees of freedom for monolithically integrating the ZnTe/GaSb DBR structure with other GaSb-based materials without generating large amounts of misfit dislocations, thus ensuring the best possible materials quality. More importantly, GaSb and ZnTe have a large refractive index contrast in the MWIR range [for example, $\Delta n = 1.18$ at 0.6 eV (Ref. 11)], which is significantly higher than that of other widely used DBRs in the MWIR range, as shown in Table I.[9,10,12–14] It was previously demonstrated that the ZnTe/GaSb DBRs could achieve a peak reflectivity of 99.0% centered at 2.5 μm with 480-nm-wide stopband.[10] In this paper, the growth of ZnTe/GaSb DBRs using molecular beam epitaxy (MBE) is described. Post-growth characterization using x-ray diffraction (XRD), atomic force microscopy (AFM), transmission electron microscopy

[a)]Electronic mail: yhzhang@asu.edu

TABLE I. Comparison between commonly used DBRs in NIR/MWIR VCSELs and ZnTe/GaSb DBRs.[9,10,12–14]

DBR materials	Refractive index contrast (Δn)	Number of pairs needed for R = 99.9% (N)	Lasing wavelength (μm)
InGaAsP/InP (Ref. 13)	0.18	65	1.3
AlGaInAs/InP (Ref. 13)	0.19	63	1.3
AlGaAsSb/AlAsSb (Ref. 13)	0.49	27	1.3
AlAs/GaAs (Ref. 13)	0.50	23	1.3
AlGaAsSb/AlAsSb (Ref. 12)	0.44	31	1.55
AlGaAsSb/InP (Ref. 12)	0.43	33	1.55
AlGaInAs/InP (Ref. 12)	0.34	38	1.55
AlGaInAs/AlInAs (Ref. 12)	0.30	43	1.55
GaInAsP/InP (Ref. 12)	0.27	51	1.55
InGaAs/InAlAs (Ref. 9)	0.27	30	2.3
AlAsSb/GaSb (Ref. 14)	0.60	22	2.5
ZnTe/GaSb (Ref. 10)	1.18	10	2.3–2.5

(TEM), and reflectance spectroscopy are carried out to comprehensively study the material properties of the ZnTe/GaSb DBRs.

II. EXPERIMENTAL DETAILS

A series of ZnTe/GaSb DBR samples with different numbers of $\lambda/4$ pairs was designed and grown using an MBE system consisting of two separate II-VI and III-V growth chambers connected by an ultrahigh-vacuum transfer module. The vacuum of the transfer chamber was kept below 5×10^{-9} Torr, preventing any cross contamination during sample transfer. The DBR structures were grown on a GaSb (001) substrate with a buffer. The substrate temperatures were measured using a thermocouple on the back of the substrate holder. During growth, the ZnTe epilayers were deposited at 320 °C in the II-VI chamber while the GaSb epilayers were grown in the III-V chamber.

The normal growth temperature for GaSb (~470 °C) is much higher than that for ZnTe (~320 °C). Therefore, the interface between ZnTe and GaSb could be severely damaged if the initial growth of GaSb on ZnTe is carried out at such a high temperature. To address this problem, a temperature ramp was introduced while GaSb was being initially deposited on ZnTe.[15] The growth temperature was gradually ramped up from 360 to 470 °C at a rate of 33 °C/min to protect the ZnTe layer surfaces and to achieve high material quality.[15] The wafers were transferred repeatedly between the II-VI and III-V chambers to complete the entire DBR structure. The growth parameters for the samples described in this paper, including growth temperatures, temperature ramping rate, beam equivalent pressure ratios, and growth rates, were reported previously.[15] The number of $\lambda/4$ pairs for each grown sample is summarized in Table II.

High-resolution XRD ω-2θ scans were carried out on a PANalytical X'Pert PRO MRD x-ray diffractometer with multicrystal monochromator. Surface morphology was studied using AFM. Cross-sectional TEM studies were carried out using a JEM-4000EX high-resolution electron microscope operated at 400 keV with a structural resolution of ~1.7 Å. Reflectance spectra were measured using a Fourier transform infrared spectrometer equipped with a CaF_2 beam-splitter and a liquid-nitrogen-cooled HgCdTe detector.

TABLE II. List of the ZnTe/GaSb DBR samples with MBE run number and the numbers of $\lambda/4$ pairs.

Sample number	MBE run number	Number of $\lambda/4$ pairs (N)
1	120412B	1
2	111122C	2
3	120412A	4
4	120313A	7
5	120413A	7
6	120314A	7

III. RESULTS AND DISCUSSION

After completion of growth, high-resolution XRD measurements were performed on the grown samples in the vicinity of the (004) diffraction peak of GaSb. The Cu $K_{\alpha 1}$ line was used as the incident beam. The (004) ω-2θ curves for the DBR samples with different numbers of $\lambda/4$ pairs (N = 1, 2, 4) are shown in Fig. 1. The diffraction peaks of ZnTe layer and GaSb substrate are clearly observed. Their peak separations ($\Delta\theta$) for all samples are listed in Table II. It is found that the $\Delta\theta$ value is slightly increased by 15 arc sec as the number of $\lambda/4$ pairs increases from N = 1 to N = 4. Correspondingly, the relative change in the lattice constant of ZnTe layers between the DBR samples of one and four $\lambda/4$ pairs is only about 0.0098%, indicating that there is only a small effect on lattice parameters and residual strain introduced by growing different numbers of $\lambda/4$ pairs. Furthermore, Pendellösung fringes are observed from all samples, indicating good interface smoothness, excellent composition, and thickness uniformities of all layers.

The ZnTe and GaSb layer thicknesses can be estimated using the separation of the Pendellösung fringes, as described by the following equation:

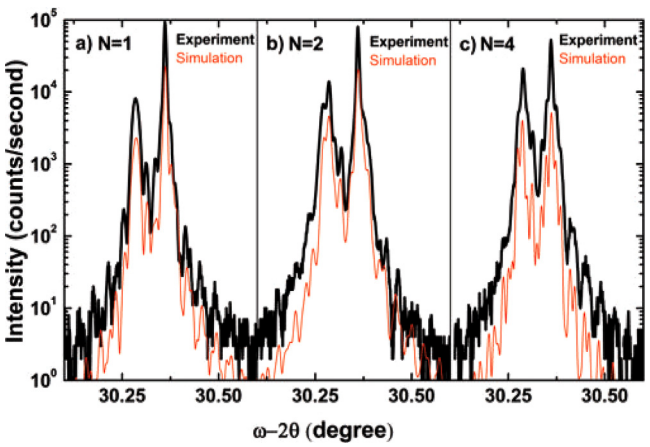

FIG. 1. (Color online) Experimental and simulated ω-2θ XRD patterns for the ZnTe/GaSb DBR samples with different number of $\lambda/4$ pairs (N): (a) N = 1; (b) N = 2; and (c) N = 4.

TABLE III. Summary of XRD measurement results of the ZnTe/GaSb DBR samples.

Sample number ($\lambda/4$ pairs)	Peak separation between ZnTe layer and GaSb substrate (arc sec)	ZnTe layer thickness (nm)	GaSb layer thickness (nm)
1 (N = 1)	274	255	145
2 (N = 2)	270	265	140
3 (N = 4)	259	270	145

$$d = \frac{\lambda}{2 \cdot \Delta\theta_P \cdot \cos\theta_B},$$

where d is the layer thickness, λ is the incident x-ray wavelength, $\Delta\theta_P$ is peak separation between Pendellösung fringes, and θ_B is the Bragg angle. The thicknesses of ZnTe and GaSb layers are then calculated for each sample as summarized in Table III. For comparison, the (004) XRD patterns for each sample are also simulated using X'PERT EPITAXY software and show close agreement with the experimental data.

AFM measurements were carried out to study the surface morphology of the grown samples. The AFM images for three samples of different $\lambda/4$ pairs (N = 1, 4, 7) were recorded over $3 \times 3\ \mu m^2$ areas, as shown in Figs. 2(a)–2(c). A well-defined step-flow growth mode is observed for all samples. The root-mean-square (RMS) surface roughness is found to be ~0.193 nm (N = 1), 0.221 nm (N = 4), and 0.691 nm (N = 7), indicating smooth surface morphology. The RMS values show that the surface roughness increases slightly as the number of $\lambda/4$ pairs increases. The results show that the observed surface and interface roughnesses of these samples have limited impact on the peak reflectivity because the wavelength of the light being reflected is much longer (~2.5 μm) than the dimensions of the roughnesses.

Cross-sectional specimens were prepared for TEM observation using mechanical polishing and dimpling followed by Argon ion-milling. As illustrated by Fig. 3, low-magnification TEM images for the ZnTe/GaSb DBR samples revealed high quality ZnTe and GaSb epilayers with a low density of interfacial defects. Smooth morphology for all of the ZnTe/GaSb and GaSb/ZnTe interfaces is clearly observed. Very few misfit dislocations and no stacking faults are visible at the interfaces, indicating highly coherent interfacial configuration and overall high crystallinity. In addition, a few dark spots are visible in the region of the GaSb buffer layer and GaSb substrate: these are caused by milling damage during sample preparation.

Reflectance measurements were performed at normal incidence using a Globar as the light source. The reflectance spectra were measured in the spectral range from NIR (~1.7 μm) to MWIR (~6.2 μm), as shown in Fig. 4. The reflectance spectra show that the peak reflectance increases quickly from 53% to almost unity as the number of $\lambda/4$ pairs increases from one to seven. The sample with seven $\lambda/4$ pairs shows best results with a peak reflectance of 99.0% at 2.56 μm and a stopband of 517-nm width. To investigate the reproducibility

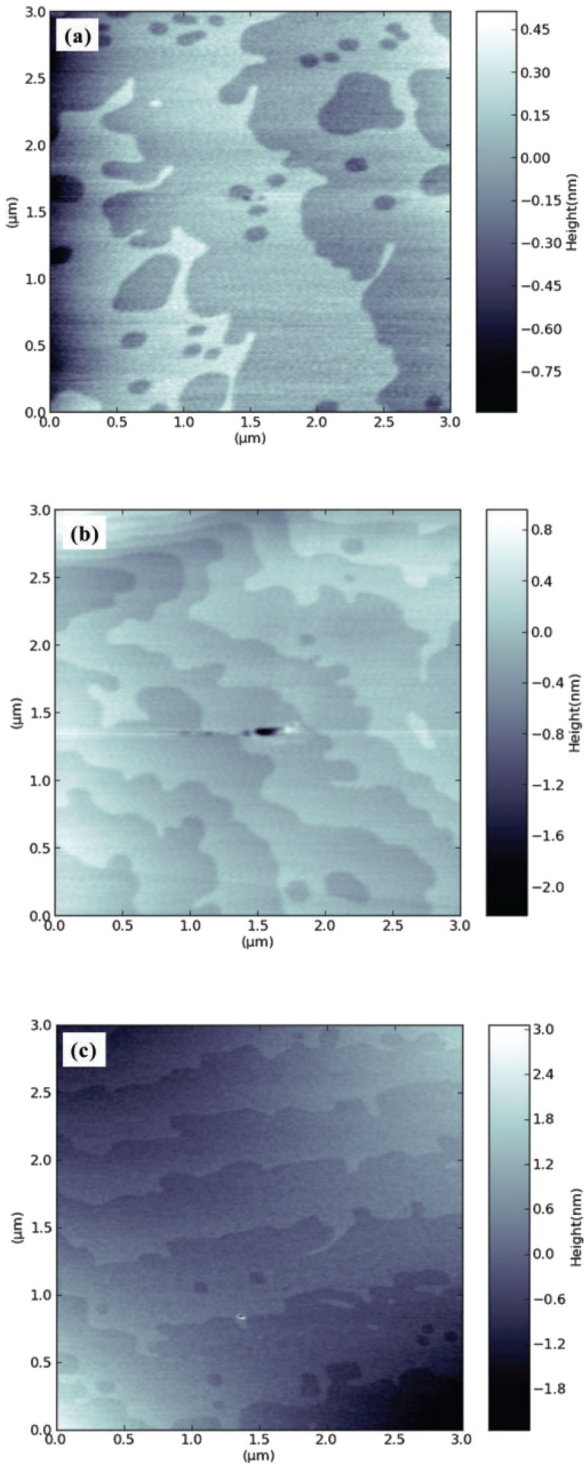

FIG. 2. (Color online) AFM images of three ZnTe/GaSb DBR samples with different number of $\lambda/4$ pairs (N): (a) N = 1; (b) N = 4; and (c) N = 7.

of the MBE growth of the samples, three different DBR samples with seven $\lambda/4$ pairs were grown and their reflectance spectra were measured and compared. The peak reflectance, stopband center wavelengths, and bandwidths of these samples are summarized in Table IV. The peak reflectance has a variation of ~2.2%, the center wavelengths of stopbands are within 70 nm, and bandwidths of stopband are within 30 nm, indicating a good reproducibility.

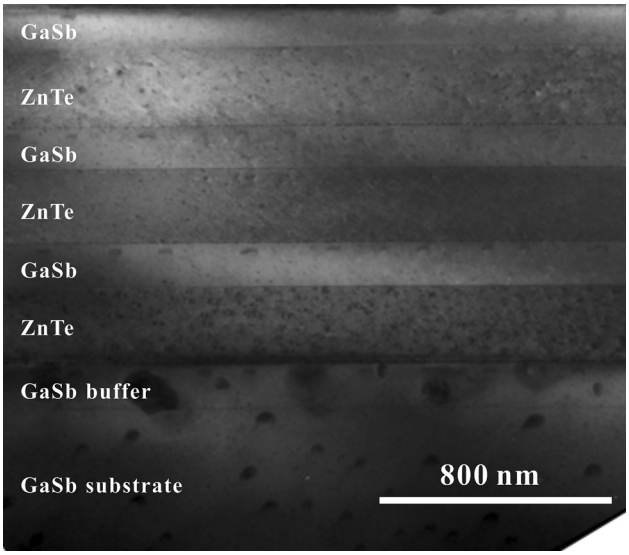

FIG. 3. Low-magnification TEM image of a ZnTe/GaSb DBR sample with seven $\lambda/4$ pairs.

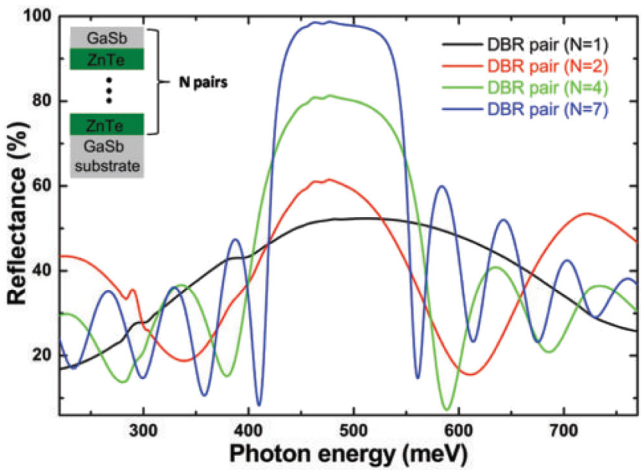

FIG. 4. (Color online) Experimental reflectance spectra for the ZnTe/GaSb DBR samples with different number of $\lambda/4$ pairs (N = 1, 2, 4, 7).

TABLE IV. Summary of reflectance results of DBR samples with seven $\lambda/4$ pairs.

Sample number ($\lambda/4$ pairs)	Peak reflectance (%)	Stopband center wavelength (μm)	Stopband bandwidth (nm)
4 (N = 7)	98.8	2.51	495
5 (N = 7)	99.0	2.56	517
6 (N = 7)	96.8	2.58	525

IV. SUMMARY

In summary, high-reflectivity and broad-bandwidth DBRs based on ZnTe/GaSb quarter-wavelength ($\lambda/4$) layers have been successfully grown on GaSb (001) substrates using MBE. During the MBE growth, GaSb layers were deposited under a temperature ramp to protect the GaSb/ZnTe interfaces and to achieve good material quality. Post-growth characterization using XRD, AFM, and TEM indicate overall excellent crystallinity, surface morphology, and highly coherent interfaces. Reflectance measurements show that a peak reflectance of 99.0% with a wide stopband of 517 nm centered at 2.56 μm is experimentally achieved from a sample with seven $\lambda/4$ pairs.

ACKNOWLEDGMENTS

The work at ASU was partially supported by a Science Foundation Arizona grant (SRG 0339-08) and an AFOSR (FA9550-10-1-0129). ASU and Notre Dame were also jointly supported by an NSF grant (ECCS-1002072). The authors gratefully acknowledge the use of facilities in the John M. Cowley Center for High Resolution Electron Microscopy, the Center for Solid State Electronics Research, and the LeRoyEyring Center for Solid State Science at Arizona State University.

[1]C. J. Chang-Hasnain, IEEE J. Sel. Top. Quantum Electron. **6**, 978 (2000).
[2]J. S. Harris, IEEE J. Sel. Top. Quantum Electron. **6**, 1145 (2000).
[3]F. Riemenschneider, M. Maute, H. Halbritter, G. Boehm, M.-C. Amann, and P. Meissner, IEEE Photon. Technol. Lett. **16**, 2212 (2004).
[4]M. Maute, B. Kögel, G. Böhm, P. Meissner, and M.-C. Amann, IEEE Photon. Technol. Lett. **18**, 688 (2006).
[5]J. J. Dudley, D. I. Babic, R. P. Marin, L. Yang, B. I. Millers, R. J. Ram, T. E. Reynolds, E. L. Hu, and J. E. Bowers, Appl. Phys. Lett. **64**, 1463 (1994).
[6]V. Jayaraman, T. J. Goodnough, T. L. Beam, F. M. Ahedo, and R. A. Maurice, IEEE Photon. Technol. Lett. **12**, 1595 (2000).
[7]L. Cerutti, A. Garnache, A. Ouvrard, M. Garcia, E. Cerda, and F. Genty, Electron. Lett. **40**, 869 (2004).
[8]A. Bachmann, T. Lim, K. Kashani-Shirazi, O. Dier, C. Lauer, and M.-C. Amann, Electron. Lett. **44**, 202 (2008).
[9]M. Ortsiefer, G. Böhm, M. Grau, K. Windhorn, E. Rönnerberg, J. Rosskopf, R. Shau, O. Dier, and M.-C. Amann, Electron. Lett. **42**, 640 (2006).
[10]J. Fan, X. Liu, J. K. Furdyna, and Y.-H. Zhang, Appl. Phys. Lett. **101**, 121909 (2012).
[11]S. Adachi, *Handbook on Physical Properties of Semiconductors Volume 2: III-V Compound Semiconductors* (Kluwer, Boston, 2004).
[12]M. H. M. Reddy, T. Asano, R. Koda, D. A. Buell, and L. A. Coldren, Electron. Lett. **38**, 1181 (2002).
[13]C.-K. Lin, D. P. Bour, J. Zhu, W. H. Perez, M. H. Leary, A. Tandon, S. W. Corzine, and M. R. T. Tan, IEEE J. Sel. Top. Quantum Electron. **9**, 1415 (2003).
[14]A. Ducanchez, L. Cerutti, P. Grech, F. Genty, and E. Tournié, Electron. Lett. **45**, 265 (2009).
[15]J. Fan, L. Ouyang, X. Liu, D. Ding, J. K. Furdyna, D. J. Smith, and Y.-H. Zhang, J. Vac. Sci. Technol. B **30**, 02B122 (2012).